Electrostatic and Hydrodynamic Orientational Steering Effects in Enzyme-Substrate Association

Jan Antosiewicz and J. Andrew McCammon
Department of Chemistry and Biochemistry, and Department of Pharmacology, University of California at San Diego, La Jolla, California 92093-0365 USA

ABSTRACT Diffusional encounters between a dumbbell model of a cleft enzyme and a dumbbell model of an elongated ligand are simulated by Brownian dynamics. The simulations take into account electrostatic and hydrodynamic interactions between the molecules. It is shown that the primary effect of inclusion of hydrodynamic interactions into the simulation is an overall decrease in the rate constant. Hydrodynamic orientational effects are of modest size for the systems considered here. They are manifested when changes in the rate constants for diffusional encounters favored by hydrodynamic interactions are compared with those favored by electrostatic interactions as functions of the overall strength of electrostatic interactions. The electrostatic interactions modify the hydrodynamic torques by modifying the drift velocity of the substrate toward the enzyme. We conclude that simulations referring only to electrostatic interactions between an enzyme and its ligand may yield rate constants that are somewhat (e.g., 20%) too high, but provide realistic descriptions of the orientational steering effects in the enzyme-ligand encounters.

INTRODUCTION

The first step in many biological processes is the diffusional encounter of ligand and receptor molecules (McCammon and Harvey, 1987). Diffusional encounter is thought to influence or limit the rate of action of a number of enzymes. The initial inference that a biochemical process is diffusion-controlled is drawn typically from the high value of the corresponding experimental bimolecular rate constant. For the enzyme-substrate association

$$E + S \xrightarrow{k} ES$$

and typical molecular sizes, the traditional Smoluchowski theory (see, e.g., Atkins, 1994), which assumes spherical reaction partners with uniformly reactive surfaces, yields a bimolecular rate constant k of about 10^{10} M^{-1} s^{-1}. However, even significantly smaller actual rate constants may be consistent with a reaction mechanism controlled by diffusion, because the rate of productive diffusional encounter will be modulated generally by the various interactions between the reaction partners and by orientational requirements for complex formation. Among the possible interactions, only electrostatic interactions (EI) usually have been considered in theoretical studies of enzyme kinetics (see, e.g., Head-Gordon and Brooks, 1987; Northrup et al., 1987; Antosiewicz et al., 1994, 1995). In some studies, the influence of hydrodynamic interactions (HI) have also been taken into account (Friedman, 1966; Deutch and Felderhof, 1973; Wolynes and Deutch, 1976; Allison et al., 1984; Northrup et al. 1984). HI result from the fact that a moving solute particle tends to move the surrounding solvent. The solvent motion, in turn, tends to displace other solute molecules. Thus, HI slow the relative motion of the reactants and, in general, lead to some decrease in the diffusional encounter rate constants.

An interesting aspect of the influence of electrostatic and hydrodynamic interactions on molecular association arises in situations where the molecules not only must be brought into close proximity, but also must be oriented correctly in space for a successful encounter (e.g., binding or reaction) to occur. The role of electrostatic torques in speeding certain enzymatic reactions has been demonstrated previously (Luty et al., 1993; Wade et al., 1994). More recently, Brune and Kim (1994) have suggested that in the case of a cleft enzyme interacting with elongated substrate, hydrodynamic steering torques could also play a significant role.

Here, we investigate the possible role of HI by performing Brownian dynamics simulations of diffusional encounter between a model of a cleft enzyme and a model of an elongated ligand. We use bead models for the enzyme and ligand, with friction forces applied to the bead centers, whereas Brune and Kim used more exact models with friction forces acting on elements of the solute surface. Thus, the first step is to show that for relative velocities of enzyme and ligand as considered by Brune and Kim, and for the same assumed dipole moments of the molecules, we get similar results for hydrodynamic torques and the electrostatic torques.

The Brownian dynamics simulations for the models considered here show that the hydrodynamic torques have only a modest effect on the preferred orientation of the ligand approaching the enzyme. The primary effect of inclusion of HI between enzyme and ligand in the Brownian dynamics simulation is a 20–30% decrease in the overall rate con-

Received for publication 31 January 1995 and in final form 3 April 1995.
Address reprint requests to Dr. Jan Antosiewicz, Department of Chemistry and Biochemistry, University of California, 9500 Gilman Drive, La Jolla, CA 92093-0365. E-mail: jantosie@chemcca9.ucsd.edu.
Dr. Antosiewicz is on leave from the Department of Biophysics, University of Warsaw, Warsaw, Poland.

0006-3495/95/07/57/09 $2.00

stant. Somewhat larger effects due to HI torques could occur in cases where HI and EI favor the same orientation, or when stronger attraction due to EI leads to larger velocities of approach. These possibilities currently are being studied.

MATERIALS AND METHODS

Theoretical basis

When solute particles translate and rotate in a viscous fluid at sufficiently small Reynolds numbers (so their movements are quasi-steady), then the forces and torques exerted by the fluid on the particles are linear functions of their translational and angular velocities (Happel and Brenner, 1973). The forces and the torques may be evaluated approximately on the basis of bead models of the particles, with each bead acting as a frictional center (Garcia de la Torre and Blomfield, 1981). These models will be used in the present work.

Consider N spherical beads immersed in a viscous solvent. When this set of beads moves in the solvent, bead i experiences the resistance force $\mathbf{f}_i$, which is related to the relative velocity of the bead through the relation

$$\mathbf{f}_i = -\zeta_i(\mathbf{u}_i - \mathbf{v}_i) \; (i = 1, 2, \ldots, N) \tag{1}$$

In the above equation, $\zeta_i = 6\pi\eta\sigma_i$ is the Stokes law friction coefficient of a sphere of radius σ_i in a solvent of viscosity η. Vector $\mathbf{u}_i$ represents the velocity of the bead in a laboratory coordinate system, and vector $\mathbf{v}_i$ represents the velocity that the solvent would have at the position of the ith bead if that bead were absent. When the solvent is at rest in the absence of the set of N beads, then $\mathbf{v}_i$ results entirely from the motion of all of the remaining spherical elements. The creation of this velocity of the solvent is known as hydrodynamic interaction (Oseen 1927; Zwanzig 1969; Happel and Brenner 1973). Because $\mathbf{f}_i$ is the frictional force exerted on the ith bead by the solvent, then $-\mathbf{f}_i$ is the force that this bead exerts on the medium. This force is assumed to be localized at the position $\mathbf{r}_i$ of the center of the bead. Now when a point force is exerted on a viscous incompressible fluid, in steady motion at low Reynolds number, it produces an extra velocity field $\Delta v(r)$ everywhere in the medium. This extra velocity field is a linear function of the force but not necessarily in the direction of the force. It can be characterized quantitatively by the equation (Zwanzig, 1969)

$$\Delta\mathbf{v}(\mathbf{r}) = \hat{\mathbf{T}}(\mathbf{r} - \mathbf{r}_i) \cdot (-\mathbf{f}_i) \tag{2}$$

with the hydrodynamic interaction tensor $\hat{\mathbf{T}}(\mathbf{r})$ determined by the equation

$$\hat{\mathbf{T}}(\mathbf{r}) = \frac{1}{8\pi\eta r}\left(\hat{\mathbf{I}} + \frac{\mathbf{rr}}{r^2}\right), \tag{3}$$

where $\hat{\mathbf{I}}$ is unit tensor (Oseen 1929). Thus, the velocity $\mathbf{v}_i$ can be expressed as

$$\mathbf{v}_i = -\sum_{j\neq i} \hat{\mathbf{T}}_{ij} \cdot f_j, \tag{4}$$

where $\hat{\mathbf{T}}_{ij} \equiv \hat{\mathbf{T}}(\mathbf{r}_i - \mathbf{r}_j)$ and it is assumed that the solvent is at rest in the absence of the particle. The Oseen tensor was modified subsequently by Rotne and Prager (1969), by Yamakawa (1970) and by Garcia de la Torre and Bloomfield (1978) to take into account the finite size of the beads, leading to the following expressions for the HI tensor

$$\hat{\mathbf{T}}_{ij} = \frac{1}{8\pi\eta r_{ij}}\left[\hat{\mathbf{I}} + \frac{\mathbf{r}_{ij}\mathbf{r}_{ij}}{r_{ij}^2} + \frac{\sigma_i^2 + \sigma_j^2}{r_{ij}^2}\left(\frac{1}{3}\hat{\mathbf{I}} - \frac{\mathbf{r}_{ij}\mathbf{r}_{ij}}{r_{ij}^2}\right)\right] \tag{5}$$

when $r_{ij} > \sigma_i + \sigma_j$, and

$$\hat{\mathbf{T}}_{ij} = \frac{1}{6\pi\eta\sigma_i}\left[\left(1 - \frac{9}{32}\frac{r_{ij}}{\sigma}\right)\hat{\mathbf{I}} + \frac{3}{32}\frac{r_{ij}r_{ij}}{\sigma r_{ij}^2}\right] \tag{6}$$

when $r_{ij} \leq 2\sigma_i$. For $i = j$, the hydrodynamic interaction tensor is

$$\hat{\mathbf{T}}_{ij} = \frac{1}{6\pi\eta\sigma_i}\hat{\mathbf{I}}. \tag{7}$$

Equation 5 is valid for nonoverlapping beads of arbitrary radii, whereas Eq. 6 is to be used for overlapping beads but the limitation is that they must be of equal size. Equations 5–7 are valid for stick boundary conditions. Analogous equations could be written for slip boundary conditions.

From Eqs. 1 and 4, one gets the following system of linear equations for the forces experienced by the beads

$$\sum_{j=1}^{N} \hat{\mathbf{Q}}_{ij} \cdot \mathbf{f}_j = -\zeta_i\mathbf{u}_i \tag{8}$$

with

$$\hat{\mathbf{Q}}_{ij} = \delta_{ij}\hat{\mathbf{I}} + (1 - \delta_{ij})\zeta_i\hat{\mathbf{T}}_{ij}. \tag{9}$$

Solving Eq. 8 for given velocities of the N beads, we obtain the forces $\mathbf{f}_i$ and torques $\mathbf{t}_i \equiv \mathbf{r}_i \times \mathbf{f}_i$ experienced by the beads. The torques depend on the choice of center of the coordinate system for determination of the position vectors of the beads, $\mathbf{r}_i$. Summing up all individual forces and torques, we obtain total hydrodynamic force $\mathbf{f}$ and torque $\mathbf{t}$ acting on the set on N beads.

The calculated hydrodynamic torque depends on the choice of origin for the coordinates of the beads forming the model of a molecule (Brenner 1964a, b). But in the case of particles with a center of symmetry, and the bead models considered in the present work have this feature, it is sufficient to refer to the centers of symmetry of each molecule. Assuming now that M beads belong to the first molecule and the remaining to the second, we can calculate the net hydrodynamic forces and torques for given velocities.

Simultaneously, we can calculate the electrostatic forces between the beads from their net charges q_i, the dielectric constant ϵ of the solvent, and the ionic strength I. One way is to solve the Poisson-Boltzmann equation and find the gradient of the potential. The second way, used by Brune and Kim (1994), is to use the model of point charges in a uniform dielectric with Debye-Hückel screening due to the ionic strength. Then the force between two charges q_i and q_j is expressed as

$$\mathbf{f}_{ij} = \frac{q_iq_j}{\epsilon r_{ij}^2}\frac{\exp(\kappa(a - r_{ij}))}{1 + \kappa a}\left(\kappa + \frac{1}{r_{ij}}\right)\mathbf{r}_{ij}, \tag{10}$$

where $1/\kappa$ is the Debye length (see, e.g., Atkins, 1994) and $a = \sigma_i + \sigma_j$ is the distance of closest approach of the ions. For a single-sphere enzyme model and single-sphere substrate model, Eq. 10 agrees exactly with solution to the Poisson-Boltzmann equation. For molecules modeled by a larger number of beads, Eq. 10 is simply an approximation in treating forces as sums due to separated single spheres. Having the forces determined according to Eq. 10 or from solution of the Poisson-Boltzmann equation, we can calculate the net electrostatic forces and torques for the molecules participating in the reaction.

In a solution, particles do not move with constant velocities. Because of constant bombardment of the solute molecules by solvent molecules, the velocity vector of each solute frequently changes its direction and value. Thus, to study the influence of electrostatic and hydrodynamic forces and torques on diffusional encounter rate constants, we make use of the Brownian dynamics simulation method.

Brownian dynamics simulations can be done with an algorithm proposed by Ermak and McCammon (1978). Consider again N beads. The first M beads form a model of the enzyme. They have radii σ_e. The remaining $N - M$ beads represent beads of the substrate. They have radii σ_s. The Brownian motion of the system of N beads in the time interval $\Delta t = t - t_o$ is described by the equation

$$\Delta\mathbf{r} = \frac{\Delta t}{k_BT}\hat{\mathbf{Q}} \cdot \mathbf{F} + \mathbf{R}(\Delta t). \tag{11}$$

In the above equation, vectors $\mathbf{r}$, $\mathbf{F}$, and $\mathbf{R}$ are $3N \times 1$ column vectors obtained by stacking the N column vectors $\mathbf{r}_i$, $\mathbf{F}_i$, or $\mathbf{R}_i$, on top of each other. The vectors $\mathbf{r}_i$, $\mathbf{F}_i$, and $\mathbf{R}_i$ describe the position, force, and random displacement of the ith bead. The matrix $\hat{\mathbf{Q}}$ is a symmetric $3N \times 3N$ supermatrix constructed from the 3×3 hydrodynamic interaction tensors $\hat{\mathbf{D}}_{ij}$ between beads i and j. Thus,

$$\hat{\mathbf{Q}} = \begin{pmatrix} \hat{\mathbf{D}}_{11} & \hat{\mathbf{D}}_{12} & \cdots & \hat{\mathbf{D}}_{1N} \\ \hat{\mathbf{D}}_{21} & \hat{\mathbf{D}}_{22} & \cdots & \hat{\mathbf{D}}_{2N} \\ \vdots & \vdots & \ddots & \vdots \\ \hat{\mathbf{D}}_{N1} & \hat{\mathbf{D}}_{N2} & \cdots & \hat{\mathbf{D}}_{NN} \end{pmatrix} \tag{12}$$

and

$$\hat{\mathbf{D}}_{ij} = k_B T \hat{\mathbf{T}}_{ij}. \tag{13}$$

The matrix $\hat{\mathbf{Q}}$ and vector $\mathbf{F}$ are evaluated at the beginning of each time step. The vector $\mathbf{R}$ representing the random steps of all beads may be obtained from

$$\mathbf{R} = \hat{\mathbf{S}} \cdot \mathbf{X}, \tag{14}$$

where, the $3N \times 3N$ tensor $\hat{\mathbf{S}}$ is derived from tensor $\hat{\mathbf{Q}}$ by the relation

$$\hat{\mathbf{Q}} = \hat{\mathbf{S}} \cdot \hat{\mathbf{S}} \tag{15}$$

and $\mathbf{X}$ is a $3N \times 1$ column vector, the elements of which are random Gaussian numbers with zero mean and $2\Delta t$ variance. Thus, finally, we may represent the Brownian motion of the set of N beads by the equation

$$\Delta \begin{pmatrix} \mathbf{r}_1 \\ \mathbf{r}_2 \\ \vdots \\ \mathbf{r}_N \end{pmatrix} = \frac{\Delta t}{k_B T} \begin{pmatrix} \hat{\mathbf{D}}_{11} & \hat{\mathbf{D}}_{12} & \cdots & \hat{\mathbf{D}}_{1N} \\ \hat{\mathbf{D}}_{21} & \hat{\mathbf{D}}_{22} & \cdots & \hat{\mathbf{D}}_{2N} \\ \vdots & \vdots & \ddots & \vdots \\ \hat{\mathbf{D}}_{N1} & \hat{\mathbf{D}}_{N2} & \cdots & \hat{\mathbf{D}}_{NN} \end{pmatrix} \cdot \begin{pmatrix} \mathbf{F}_1 \\ \mathbf{F}_2 \\ \vdots \\ \mathbf{F}_N \end{pmatrix} + \begin{pmatrix} \hat{\mathbf{S}}_{11} & \hat{\mathbf{S}}_{12} & \cdots & \hat{\mathbf{S}}_{1N} \\ \hat{\mathbf{S}}_{21} & \hat{\mathbf{S}}_{22} & \cdots & \hat{\mathbf{S}}_{2N} \\ \vdots & \vdots & \ddots & \vdots \\ \hat{\mathbf{S}}_{N1} & \hat{\mathbf{S}}_{N2} & \cdots & \hat{\mathbf{S}}_{NN} \end{pmatrix} \cdot \begin{pmatrix} \mathbf{X}_1 \\ \mathbf{X}_2 \\ \vdots \\ \mathbf{X}_N \end{pmatrix}. \tag{16}$$

Equation 16 forms a basis for an algorithm for simulation of the diffusional motion of an enzyme and substrate, with hydrodynamic interactions between them included.

Software

The Brownian dynamics simulations described in this work are done using the UHBD program (Davis et al., 1991; Madura et al., 1994). In version 4.1 of UHBD, an algorithm based on Eq. 16 is used to include hydrodynamic interactions only between subunits of diffusing substrate. HI between subunits of the enzyme are neglected. Diffusion of enzyme, without taking HI with the ligand into account, is included through the effective hydrodynamic radius r_E of the enzyme, by adding $kT/6\pi\eta r_E$ to the diffusional coefficients of subunits of the ligand.

The basic change introduced in UHBD for the purpose of the present work was to allow hydrodynamic interactions between all subunits of the enzyme and the substrate. All subunits now move according to Eq. 16. At the end of each step, the displacement of the enzyme's subunits are used to find the net translational displacement of the center of the enzyme. This net displacement is subtracted from the displacements of all subunits of substrate, and the enzyme is reset to its initial location. Thus, in effect we do not consider the rotational motion of the enzyme, which is a reasonable approximation here because of the relatively large size of the enzyme.

The next important point relates to the forces exerted by the substrate's subunits on the enzyme's subunits. In the original version of UHBD, the Poisson-Boltzmann equation is solved for the enzyme, and subunits of substrate are treated as test charges. Forces are calculated from the gradient of the potential around the enzyme. From Eq. 16, it is obvious that we also need forces on the enzyme's subunits. Calculation of all of the forces by solving the Poisson-Boltzmann equation for both enzyme and substrate, for all steps on Brownian dynamics trajectory, currently is not possible because of the computational cost of such a simulation. Thus, we do the following. The force exerted by the substrate on the enzyme has the same magnitude as the force exerted by the enzyme on the substrate, but has opposite direction. We need to distribute this force among the individual subunits of the enzyme. To do this, we calculate the forces exerted on the enzyme's subunits by the substrate subunits, according to Eq. 10.

Assume that the net force on the enzyme, resulting from Eq. 10, is $\mathbf{F}_E$. This force is usually not equal to $-\mathbf{f}_S$, the force on the substrate resulting from gradient of the potential around the enzyme, because it was obtained differently, i.e., not from the finite difference solution of the Poisson-Boltzmann equation. But now the assumption is made that the component forces on different subunits of the enzyme that would result from solution of the full Poisson-Boltzmann equation are in the same relation to each other as component forces calculated by Eq. 10, which lead to $\mathbf{F}_E$. We therefore modify the forces on the subunits of the enzyme, calculated by Eq. 10, according to the following rule: if the component of $\mathbf{F}_E$ along the ith axis is not zero, the ith component of the electrostatic force exerted on the given subunit of the enzyme is corrected by the factor $-\mathbf{f}_{S,i}/\mathbf{F}_{E,i}$. If the component of $\mathbf{F}_E$ along the ith axis is zero, then the ith component of the electrostatic force exerted on the given subunit of the enzyme is corrected by addition of $-\mathbf{f}_{S,i}/M$, where M is the number of enzyme's subunits. With this rule, the resulting forces on the subunits of enzyme are proportional to their charges and take into account distances to different parts of the ligand, and the total sum of the forces acting on the enzyme's subunits is always $-\mathbf{f}_S$ as it should be. It seems that the only better (and actually correct) alternative to this algorithm would be to solve the Poisson-Boltzmann equation each time step in Brownian dynamics simulation for the whole enzyme-substrate system.

The approximate description of forces given above is strictly correct for single-bead enzyme and single-bead substrate, and is expected to be reasonable for multibead models of enzyme and substrate. For our dumbbell model of the enzyme and dumbbell model of the substrate, the result is also very reasonable, as shown in Table 1. This table provides a comparison of electrostatic forces calculated in UHBD and by a simple program based on Eq. 10. Beads 1 and 2 belong to the enzyme, and beads 3 and 4 belong to the substrate. Calculation by UHBD means that the forces on the substrate beads are calculated by original UHBD code, and forces on the enzyme beads by the procedure described above and implemented in the UHBD code. Because UHBD treats the charges of the ligand as a set of point charges, we put the distance of closest approach in Eq. 10 equal to radius of the enzyme model beads, i.e., 20 Å. As the two examples in the table show, results of calculations for different, randomly sampled positions of dumbbell ligand, one on a 80-Å sphere and one on a 60-Å sphere, are almost the same for UHBD and Eq. 10.

The last important modification of UHBD concerns a way of counting successful encounters. Because we are interested in the orientation of ligand as it approaches the enzyme, two reaction criteria are applied, one for encounters with the long axis of the substrate parallel to that of the enzyme and one for the perpendicular orientation. A trajectory is considered successful and is terminated upon satisfying either criterion. The rate constant for "parallel" encounters, for example, is therefore somewhat different than one would obtain in the absence of the "perpendicular" reaction criterion. Comparison of the "parallel" and "perpendicular" rate constants provides a measure of the orientational steering effects within a single set of trajectories.

Models

Hydrodynamically, the enzyme is modeled as two 20-Å spheres with centers separated by 50 Å. The substrate is modeled as two 5-Å spheres with centers separated by 30 Å. These models will show some quantitative differences in hydrodynamic effects in comparison with the models used by Brune and Kim, simply because friction forces act on the centers of beads and on the surface elements, respectively, in these models. But, as

TABLE 1 Comparison of electrostatic forces on beads of the enzyme and ligand models calculated in the UHBD program and according to Eq. 10

No. of bead	Forces exerted on beads					
	UHBD			Equation (10)		
	x	y	z	x	y	z
	r_b = 80Å: (21.51, −52.91, 54.23) & (36.46, −68.00, 33.05)					
1	46.56	−122.1	77.33	46.45	−121.5	76.86
2	0.34	−0.43	−0.17	0.34	−0.43	−0.17
3	−58.55	144.4	−78.79	−58.16	143.1	−78.26
4	11.65	−21.79	1.63	11.37	−21.21	1.58
	r_b = 60Å: (24.12, −64.72, −6.91) & (−3.30, −52.98, −3.72)					
1	27.50	248.5	133.7	26.66	239.4	131.1
2	50.24	−405.6	167.0	−48.69	−390.7	163.8
3	11.12	−29.95	29.44	10.80	−28.98	28.92
4	11.62	187.0	−330.1	11.24	180.3	−323.8

Forces are in 10^{-12} dyn. Beads of the enzyme have coordinates (0., 0., 25.0) and (0., 0., −25.0) (Å).

discussed below, similar results are obtained for the cases considered here. The mean translational diffusion coefficient of our enzyme model corresponds to a sphere of radius 28.6 Å, and the mean translational diffusion coefficient of our substrate model corresponds to a sphere of radius 8.6 Å. We also do some Brownian dynamics simulations with such spheres. We considered uncharged spheres, spheres with +10 units of elementary charge, and spheres with 10 units of elementary charge but of opposite signs.

Regarding the electrostatic properties of the dumbbell models, we consider two cases. In the first case, the total charges for the models are zero but both have dipole moments of 300 Debye units as imposed by Brune and Kim. Thus, the enzyme has charges of +1.25 and −1.25 at centers of its beads, and the corresponding charges for the substrate are +2.08 and −2.08. In the second case, we consider a ligand having +0.5 units of elementary charge on each of its two beads, and several models of the enzyme with −1.0, −2.0, −5.0, and −10.0 units of elementary charge on each of its beads. Thus, the maximal total charge of our enzyme model is −20 e, which may seem unrealistically large. But we should take into account that the charges of our enzyme model are at the centers of 20-Å beads, whereas the charges of real proteins are usually close to their surfaces.

Our models of enzyme and substrate are shown in Fig. 1. In this figure, the x axis is directed toward the reader, and the y and z axes are in the plane of the figure. The centers of the models are separated along the x axis by 28 Å, and the centers of enzyme's beads are on the y axis, symmetrically placed 25 Å from the origin of the coordinate system. The centers of the ligand's beads are on a line going through a point on the x axis 28 Å from the center of the coordinate system, and making angle of 40° with the z axis; the ligand's beads are symmetrically situated with respect to the x axis. This arrangement corresponds to that for which Brune and Kim presented values of the hydrodynamic torques. The calculated torques on the enzyme and ligand for this arrangement have nonzero x components only, because of symmetry. If this component for the ligand is positive, it means that the torque tends to orient the ligand perpendicularly to the enzyme. A negative torque on the enzyme means that the torque tends to orient the enzyme perpendicularly to the ligand.

Criteria for diffusional encounter

For the models considered here, the electrostatic and hydrodynamic torques favor two different relative orientations of approaching enzyme and substrate. Both orientations are shown in Fig. 2, *A* and *B*. The hydrodynamic torque tends to orient the ligand perpendicularly to the axis of the enzyme, whereas the electrostatic torque tends to orient the ligand along the axis of the enzyme. Thus, we consider the two following reaction criteria:

1) For diffusional encounter in a perpendicular arrangement, we require that the beads of the ligand are simultaneously within a given distance $D1$ from each of the beads of the enzyme.

2) For a diffusional encounter in a parallel arrangement, we require that the bead of the ligand with negative charge is within a distance $D2$ of the bead of the enzyme with positive charge, and the bead of the ligand with positive charge is within $D2$ of the bead of the enzyme with negative charge. To avoid perpendicular arrangements satisfying these requirements, we introduce dummy atoms at the ends of the enzyme, and we require that each bead of the substrate has to be not more than $D3$ from the appropriate dummy atom. For models with equal charges on the enzyme's beads, and equal charges on the ligand's beads, both parallel arrangements are equivalent.

Values of distances $D1$, $D2$, and $D3$ were chosen empirically by performing Brownian dynamics simulations and determining the rate constants for uncharged enzyme and ligand with no hydrodynamic interac-

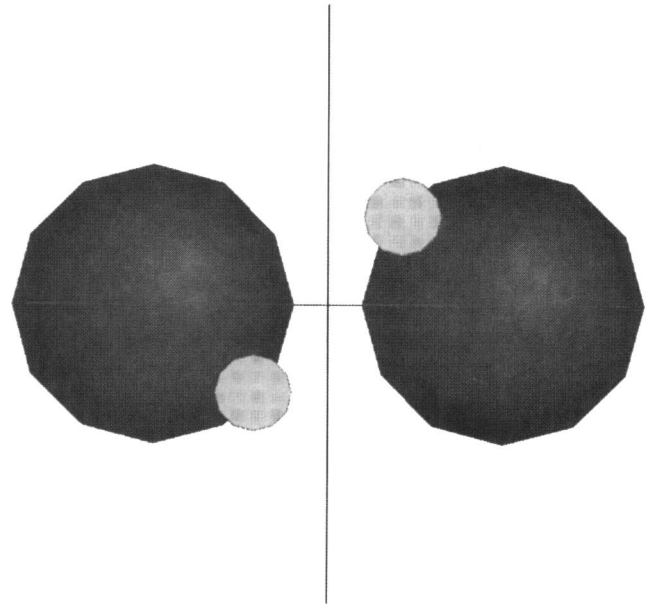

FIGURE 1 Schematic representation of the models of a cleft enzyme and an elongated ligand used in the present work. The relative orientation of the enzyme and the ligand is as for the calculation of the hydrodynamic and electrostatic torques in one of the situations considered by Brune and Kim (1994) (see text for details).

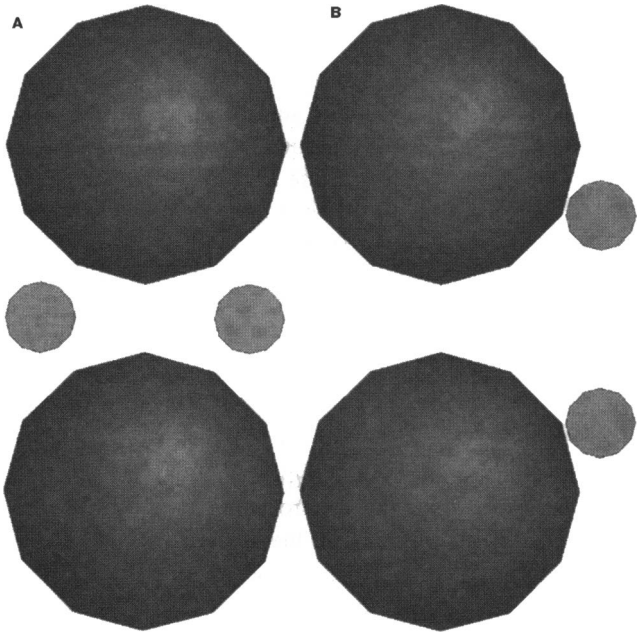

FIGURE 2 Examples of orientations of enzyme and ligand models satisfying the perpendicular (A) and parallel (*B*) reaction criteria.

tions. We tried several values of the distances and chose those for which the total number of reactions was about 10% of the number of trajectories, and the number of perpendicular reactions and parallel reactions were approximately equal. Moreover, for these distances the reaction criteria have to be mutually exclusive, i.e., a position of the ligand satisfying the perpendicular criterion cannot satisfy simultaneously any of the parallel criteria. We arrived at the following values for reaction distances satisfying the above restrictions: $D1$ = 32.0 Å, $D2$ = 31.0 Å, and $D3$ = 43.0 Å. For these values, perpendicular reactions occur for 5.2% of the trajectories, and parallel reactions occur for 4.2% of the trajectories (thus, in total, 9.4% of the trajectories yielded reactions). Fig. 3 shows the volumes available for centers of beads of the ligand that satisfy perpendicular and parallel reaction criteria, and the 25-Å spheres that represent the volume not available to the centers of beads of the ligand.

With these reaction criteria, the maximum angle between the long axis of the ligand model and long axis of the enzyme model for a parallel reaction is 72°. Decreasing the distance $D3$ leads to a decrease in this angle, but also to significant reduction in number of parallel reactions. The minimum angle between the axes for which the encounter is still classified as perpendicular is 77°; thus, the criteria are exclusive.

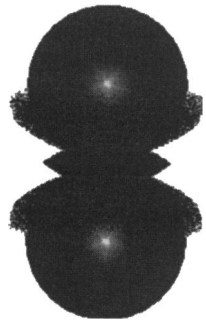

FIGURE 3 Volumes corresponding to ligand bead centers in orientations that satisfy the parallel encounter criteria (dotted volumes partly covering spheres), and the perpendicular encounter criteria (dotted volume between the spheres). The spheres represent the volume excluded to the ligand bead centers due to collisions with the enzyme.

For enzyme and ligand bearing opposite charges on the beads within each molecule, there are two different possible parallel arrangements. We call the one with the dipole moments in opposite directions "antiparallel" and that with the dipole moments in the same directions "parallel."

For simulations with spheres that have the same mean translational diffusion coefficients as our dumbbell models, we use several simple encounter criteria based on the distance between the centers of the spheres. We choose the distances such that the space between surfaces of the spheres ranges between a few Angstroms to a fraction of an Angstrom.

Summary of the Brownian dynamics simulation method

The bimolecular rate constant, k, for diffusional encounter between an enzyme and its ligand can be represented as (Madura et al., 1994):

$$k = k(b) \cdot \beta \tag{17}$$

where $k(b)$ is the rate at which the ligand initially reaches a spherical surface of radius b centered on the enzyme. If b is chosen large enough that the potential of mean force U between the reactants is centrosymmetric for distances larger than b, then $k(b)$ can be found by solving the one-dimensional diffusion equation, leading to

$$k(b)^{-1} = \int_b^\infty \frac{e^{U(r)/k_BT}}{4\pi D r^2}\,dr \tag{18}$$

where k_BT is Boltzmann's constant multiplied by temperature and D is the relative diffusion coefficient. The quantity β is the probability that a ligand started at random location on the "b surface" will reach the active site of the enzyme. This probability is estimated by generation of a large number of Brownian dynamics trajectories of the ligand around the enzyme and finding the fraction of trajectories that end with encounter (Madura et al., 1994). All Brownian dynamics trajectories are started at randomly chosen positions on the sphere of radius b and are terminated after successful encounter with the enzyme, or when they reach the surface of a "quit" sphere with radius $q > b$. There is another sphere used during simulations, namely, a sphere of radius $p < b$. When the ligand is inside the p sphere, the reaction criteria are checked after each Brownian dynamics step.

Technical details of the simulations

For runs with no EI, we did Brownian dynamics simulations on a 40 × 40 × 40 cubic grid with spacing 4.0 Å. For calculations with EI, we used a 65 × 65 × 65 cubic grid with spacing 2.5 Å. The radius of b sphere is 80.0 Å, the radius of p sphere is 65.0 Å, and the radius of q sphere is 160.0 Å.

We used a variable time step. For cases without EI, the time step is 10 ps for distances of the center of the ligand to center of the enzyme smaller than 65 Å, between 65 and 70 Å it is 100 ps, between 70 and 80 Å it is 500 ps, and for distances larger than 100 Å it is 1000 ps. With EI included and ionic strength 150 mM, these time steps are 1, 20, 80, and 500 ps, respectively. With EI included and ionic strength 10 mM, these times are 0.5, 20, 50, and 150 ps. These time intervals lead to spatial steps of the order of a fraction of an Angstrom inside the p sphere.

We used the modified Oseen hydrodynamic interaction tensor with stick boundary conditions. Overlapping between beads of the enzyme and the substrate is not allowed.

For runs with no EI, and for EI cases with neutral but dipolar enzyme and ligand, we did 60,000 trajectories. For calculations with charged enzyme and charged ligand, we did 21,000 trajectories. For single-sphere models for ligand and enzyme, we did 60,000 trajectories for each case.

Our simulations refer to a temperature of 300 K and ionic strength 150 or 10 mM. The solvent dielectric constant is set to 78, and the enzyme's dielectric constant is set to 2.

Tests of the algorithms and code

The modifications introduced into the UHBD code, and our programs for the calculation of hydrodynamic and electrostatic forces and torques, were checked by comparison with published results (Friedman, 1966; Teller et al., 1979; Allison et al., 1984; Northrup et al., 1984; Brune and Kim, 1994).

For spherical models of enzyme (σ = 6 Å) and substrate (σ = 1 Å), we find from our Brownian dynamics simulation that introduction of HI decreases the rate constant by about 15% (reaction distance 7.1 Å), both for uncharged and charged molecules (−1 and +1 units of elementary charge). These results agree well with work by Friedman (1966).

Electrostatic forces calculated in the UHBD program agree within 0.2% with the electrostatic forces calculated according to Eq. 10.

The diffusional encounter rate constants for parallel and perpendicular reaction criteria do not depend on which criterion is checked first. Thus, our reactions are exclusive.

For runs without HI, our results with modified and with original UHBD code are the same.

RESULTS

Hydrodynamic and electrostatic torques for dumbbell models

As a first step, we use bead models analogous to the system considered by Brune and Kim (1994). Our enzyme looks exactly like that of Brune and Kim. Our ligand is composed of two beads with 5-Å radii, separated by 30 Å; thus, the total length of the model of the ligand is 40 Å. The Brune and Kim model for the ligand was a capsule, 40 Å long and 10 Å in diameter. Our models have somewhat higher translational diffusion coefficients than the models used by Brune and Kim. In principle, we could correct for these effects by increasing the radii of beads, but this is not necessary for the purposes of the present work.

In Table 2, we present the calculated torques for the same velocities of both partners as considered by Brune and Kim, for 28-Å separation between their centers and for 40° skew angle between their axes. We see that our torques on the enzyme are slightly larger, and our torques on ligand are 1.8–2.8 times smaller than corresponding torques obtained by Brune and Kim. Thus, when enzyme and ligand are approaching each other with the velocities indicated above, the torques are -1.787×10^{-12} dyn cm for the enzyme and 0.616×10^{-12} dyn cm on the substrate. These torques tend to orient the approaching molecules perpendicular to each other.

For the same arrangement as described above and for charges on the enzyme and ligand resulting in permanent dipole moments of 300 Debye units, we get for electrostatic torques $+0.500 \times 10^{-14}$ dyn cm for the enzyme and -0.500×10^{-14} dyn cm for the ligand, respectively. This is for parameter a equal to the sum of radii of the enzyme beads and ligand beads. If a is equal to the radius of enzyme beads, which corresponds more closely to the algorithm used in the UHBD software, then the absolute value of the torque is slightly smaller, 0.312×10^{-14} dyn cm. These results are close to the values given by Brune and Kim for the 40° angle between enzyme and substrate axes in their Table 7. What is important for comparing with the results of Brune and Kim is that, for the conditions described above, the hydrodynamic torque on the enzyme is more than 300 times larger than corresponding electrostatic torque, and the hydrodynamic torque on the ligand more than 100 times larger than corresponding electrostatic torque. The hydrodynamic torques tend to orient the approaching particles in a perpendicular arrangement, whereas the electrostatic torque tends to orient the particles with an antiparallel arrangement of their dipole moments. It should be noticed, however, that the net electrostatic forces (3.89×10^{-8} dyn for the greater value of the parameter a and 28-Å distance between centers of enzyme and ligand) give a limiting mean translational velocity of 0.72 cm/s for the enzyme and 2.39 cm/s for the ligand. The instantaneous velocities of enzyme and ligand, calculated from the equipartition principle by Brune and Kim, are much larger. But because of the Brownian character of the solute motion, the equipartition velocities should not be used to estimate the approach velocity of two solute molecules. This can be illustrated by another estimate of the average velocity of mutual approach of enzyme and substrate, namely, the mean radial velocity found for successful Brownian dynamics trajectories. This leads to drift velocities of the ligand model between 11 and 16 cm/s for all cases (HI/EI). When this range of velocities is used to estimate the effect of hydrodynamic torque, say 15 cm/s for the ligand and 3 cm/s for the enzyme, we find that the total torque on the enzyme is -0.709×10^{-14} dyn cm, and the total torque on the substrate is 0.244×10^{-14} dyn cm. These are both comparable with the electrostatic torques. Obviously, the last estimate of mutual velocity also may not be perfectly accurate, but all necessary effects should be included when we simulate enzyme-ligand encounter by Brownian dynamics method.

TABLE 2 Comparison of torques exerted on enzyme and substrate for the model described in the text with the results of Brune and Kim for an analogous system

Velocity		Torque exerted			
		enzyme		substrate	
enzyme	substrate	This work	Brune and Kim	This work	Brune and Kim
0	3750	−1.440	−1.34	0.416	1.14
780	0	−0.347	−0.31	0.200	0.36

Velocities are in cm/s, and torques are in 10^{-12} dyn cm. Because of symmetry, the y and z components of torques are zero; the values given are x components.

TABLE 3 Comparison of diffusional encounter rate constants (in units of 10^9 M^{-1} s^{-1}) with and without HI included, for spherical models of enzyme and ligand, and for different charge models, as a function of the distance between the centers of the spheres assumed to satisfy the reaction criterion

Reaction distance (Å)	Enzyme and ligand charges					
	Without HI			With HI		
	0 0	−10 +10	+10 +10	0 0	−10 +10	+10 +10
39.0	11.04 ± 0.05	12.28 ± 0.05	9.23 ± 0.06	8.49 ± 0.05	9.68 ± 0.04	7.00 ± 0.05
38.0	10.68 ± 0.05	12.15 ± 0.05	8.50 ± 0.06	8.13 ± 0.05	9.56 ± 0.04	6.39 ± 0.05
37.5	10.38 ± 0.05	12.04 ± 0.05	7.87 ± 0.06	7.88 ± 0.05	9.46 ± 0.04	5.89 ± 0.05
37.25	10.20 ± 0.06	11.96 ± 0.05	7.40 ± 0.06	7.71 ± 0.05	9.39 ± 0.04	5.53 ± 0.05

The first charge given is that of the enzyme. The rate constants are for 60,000 trajectories.

Rate constants of diffusional encounter for spheres analogous to dumbbell models

As mentioned above, a 28.6-Å sphere has the same diffusion constant as our dumbbell model of the enzyme, and an 8.6-Å sphere has the same diffusion constant as our dumbbell model of the ligand. Thus, it is of interest to calculate the encounter rate constants for such spheres and to explore the influence of the hydrodynamic interactions and electrostatic interactions between them.

Results of our Brownian dynamics simulations for this case are presented in Table 3. First, it can be seen that in the absence of EI, hydrodynamic interactions lead to a decrease ranging from 23.1% (for reaction distance of 39 Å) to 24.4% (for reaction distance 37.25 Å) in the encounter rate constant. This is more than the 15% decrease obtained for smaller spheres as described in Materials and Methods, but this result should be expected because for spheres of larger radii the HI are stronger. We then added charges of absolute value of 10 units of elementary charge in the centers of our spheres to check how the above results change when there is also electrostatic attraction or repulsion between the spheres. For attractive EI, the decrease caused by HI ranges from 21.2 to 21.5% for the above mentioned reaction distances. For repulsive EI, these numbers range from 24.2 to 25.3%.

Brownian dynamics with dumbbell models: molecules with zero net charge

Table 4 presents calculated diffusional encounter rate constants for our models of enzyme and substrate having dipole moments of 300 Debye units at ionic strengths of 150 and 10 mM. As a reference, diffusional encounter rate constants for uncharged beads of enzyme and substrate are also presented. Changing the ionic strength from 150 to 10 mM effectively increases the electrostatic attraction between the enzyme and substrate models.

In Table 4, parallel and antiparallel reactions are distinguished; this has a physical meaning only for the molecules with permanent dipole moments. For uncharged beads, the rate constants for parallel and antiparallel arrangement should be equal. In the case of no EI, the sum of the parallel and antiparallel reactions leads to the rate constants 1.72 ± 0.05 for no HI, and 1.31 ± 0.04 for HI. All rate constants are in units of 10^9 M^{-1} s^{-1}.

Examination of the results for the no EI cases shows that HI first of all reduce the rate constants of diffusional encounter for both perpendicular and parallel encounter criteria. For the perpendicular criterion, the decrease is to 80% of the no HI value, and for parallel criteria, the decrease is to 76% of the no HI value. Taking into account 90% confidence level errors, the true value of the decrease for perpendicular reaction should be between 75 and 84%, and for parallel reactions should be between 72 and 81%. Thus, to support the conclusion that HI leads to a proportionally larger decrease of reactions not favored by HI, torques would require more trajectories; but a small effect of this kind is likely.

A comparison of the effects of hydrodynamic and electrostatic torques can be made by studying the behavior of encounter partners with permanent dipole moments, as a

TABLE 4 Comparison of diffusional encounter rate constants (in units of 10^9 M^{-1} s^{-1}) for perpendicular, antiparallel, and parallel criteria, for different models of the hydrodynamic interactions (HI) and electrostatic interactions (EI)

Presence of		Rate constant for encounter			Ionic str. (mM)
HI	EI	Perpendicular	Antiparallel	Parallel	
no	no	2.12 ± 0.06	0.88 ± 0.03*	0.88 ± 0.03*	
yes	no	1.69 ± 0.05	0.67 ± 0.03‡	0.67 ± 0.03‡	
no	yes	2.22 ± 0.06	1.03 ± 0.04	0.92 ± 0.04	150
yes	yes	1.76 ± 0.05	0.74 ± 0.03	0.68 ± 0.03	150
no	yes	2.27 ± 0.06	1.30 ± 0.05	0.76 ± 0.04	10
yes	yes	1.79 ± 0.05	0.94 ± 0.04	0.55 ± 0.03	10

*Original rates are 0.85 ± 0.04 and 0.90 ± 0.04; the data in the table have been symmetrized.

‡ Original rates are 0.70 ± 0.04 and 0.63 ± 0.03.

The rate constants are for 60,000 trajectories.

TABLE 5 Enzyme-substrate interaction energies for the two orientations shown in Fig. 2, as functions of enzyme's charge q_{enzyme}

q_{enzyme}	$E_{\perp}$ (kcal/mol)	$E_{\parallel}$ (kcal/mol)
0	0	0
−2.	−0.0155	−0.0155
−4.	−0.0309	−0.0310
−10.	−0.0774	−0.0776
−20.	−0.1547	−0.1551

The charges of enzyme's beads are equal, so that both parallel orientations have the same energy. The charge of each of the beads of the substrate is +0.5 e.

function of ionic strength. When HI are not included in the simulations, introduction of EI leads to a 5 and 7% increases in the rate constant for perpendicular encounter for 150 and 10 mM ionic strength, respectively. For antiparallel reaction, these increases are 17 and 48%, respectively. For simulations with HI included, these increases are 4 and 6% for perpendicular encounter, and 10 and 40% for antiparallel encounter, for 150 and 10 mM ionic strengths, respectively. Thus, we see that for both perpendicular and antiparallel encounters, the increase of the rate constants caused by electrostatic attraction is more pronounced for the no HI case than for the HI case. But simultaneously in both cases, no HI and HI, the increase in the rate for antiparallel encounters is more pronounced. We can also consider how the inclusion of HI changes the various rate constants. For 150 mM ionic strength, introduction of HI leads to 79% of the no HI value for perpendicular reaction and 72% of the no HI value for antiparallel encounter. For 10 mM ionic strength, these numbers are again 79 and 72%, respectively. Thus, similarly to the no EI case, we observe that introduction of HI has a slightly larger decreasing effect on antiparallel reactions than on perpendicular reactions. The effect is larger than for the no EI case and can be understood as a manifestation of hydrodynamic torque effects. But these effects are of modest importance for these particular models.

The present models yield rate constants for parallel reactions (with dipole moments in the same direction) that are only slightly smaller than for antiparallel reactions. This is because the electrostatic interaction energies are not large for these systems. The energy difference for parallel versus antiparallel orientations (Fig. 2 *B*), when the centers of the enzyme and ligand beads are separated by 25.03 Å, is 0.14 kcal/mol at 150 mM ionic strength and 0.34 kcal/mol at 10 mM ionic strength.

Brownian dynamics with dumbbell models: molecules with net charge

It seemed possible that larger torque effects due to HI would occur for oppositely charged enzyme and substrate, because the electrostatic attraction between these molecules should produce larger velocities of approach. Enzymes may bear quite significant net charge, whereas substrates usually bear small net charge. Thus, we consider models of ligand with unit positive charge, and several models of enzymes with negative charges at the centers of their beads, ranging from −1 to −10 units of elementary charge. The largest value results in a total charge of the enzyme model of −20 units of elementary charge. This might seem rather large, but the effects produced by such charges should be quite realistic, because our enzyme charges are centered inside 20 Å-beads, and our ligand is built from 5-Å beads; thus, the effect of the electrostatic interactions is expected to be smaller than in real systems, where the charges are typically on the surface of molecules. One might expect that this model increasingly favors parallel encounter orientations with increasing negative charge of the enzyme. But Table 5 shows that the perpendicular and parallel orientations are electrostatically equally probable for all charges of the enzyme model. Therefore, by increasing the charge of the enzyme model, we should observe stronger increases in the rate constant for perpendicular reactions than for parallel reactions, provided that effects of hydrodynamic torques are significant.

The results of Brownian dynamics simulations for these models with 150 mM ionic strength are presented in Table 6. The data in this table are somewhat noisy. Nevertheless, a clear increase in the total rate constant as a function of the enzyme's charge is visible. But perpendicular encounters do not dominate parallel encounters, even for the highest charges of the enzyme. On the other hand, when we evaluate the decreases caused by HI in the rate constants for perpendicular and parallel encounters, we find the following results. For perpendicular encounters, introduction of HI

TABLE 6 Comparison of diffusional encounter rate constants (in units OD 10^9 M^{-1} s^{-1}) for perpendicular, both parallel, and the all three reaction criteria, with HI and without HI, as functions of charge of the enzyme model

Charge of enzyme	Without HI			With HI		
	Perpendicular	Parallel	Total	Perpendicular	Parallel	Total
0	2.12 ± 0.06	1.72 ± 0.05	3.68 ± 0.07	1.69 ± 0.05	1.31 ± 0.04	2.89 ± 0.06
−2.	2.27 ± 0.10	1.85 ± 0.09	3.94 ± 0.12	1.81 ± 0.08	1.40 ± 0.08	3.08 ± 0.10
−4.	2.12 ± 0.10	2.02 ± 0.10	3.95 ± 0.12	1.85 ± 0.08	1.33 ± 0.07	3.05 ± 0.10
−10.	2.33 ± 0.10	2.18 ± 0.10	4.28 ± 0.12	1.85 ± 0.08	1.53 ± 0.08	3.24 ± 0.10
−20.	2.42 ± 0.10	2.27 ± 0.10	4.44 ± 0.12	1.99 ± 0.09	1.62 ± 0.08	3.45 ± 0.10

Ligand model has always charges +0.5 e on each of its beads. The rate constants are for 60,000 trajectories for no charge case and for 21,000 trajectories for each case with charged enzyme.

produces rates that range from 80 to 82% of the no HI case, when we change the charge of the enzyme from −2 to −20. For parallel encounters, the corresponding range is 76–71%. The favoring of perpendicular encounters with increasing charge when HI are included shows that hydrodynamic torques can bias the orientations of encounter, as predicted by Brune and Kim (1994). But the effects are modest even when net charges of opposite sign are present on enzyme and substrate. This is because the average velocities of encounter (10–20 cm/s in these cases) are not large.

DISCUSSION

Hydrodynamic interactions lead to a moderate decrease in the diffusional encounter rate constants for the enzyme and substrate models considered here. The extent of this decrease, in comparison with the case with no HI, depends on the size of encounter partners and also on geometry of the encounter partners.

For cleft enzymes and elongated substrates, torques arising from HI are found to favor encounters in which the long axes of the molecules are perpendicular, as suggested by Brune and Kim (1994). But this effect is much weaker than electrostatic steering effects, because of the small average velocities of enzyme-substrate encounter. It is possible that orientational steering due to HI is more significant when this operates cooperatively with electrostatic steering, and that a more accurate treatment of the hydrodynamic boundary conditions would lead to larger HI steering effects. These possibilities will be studied in further work.

We thank Professor Sangtae Kim for stimulating discussions.
This work was supported in part by National Institutes of Health and the Metacenter Program of the National Science Foundation supercomputer centers.

REFERENCES

Allison, S. A., N. Srinivasan, J. A. McCammon, and S. H. Northrup. 1984. Diffusion-controlled reactions between a spherical target and dumbbell dimer by Brownian dynamics simulation. *J. Phys. Chem.* 88:6152–6157.

Antosiewicz, J., M. K. Gilson, and J. A. McCammon. 1994. Acetylcholinesterase: effects of ionic strength and dimerization of the rate constants. *Israel J. Chem.* 34:151–158.

Antosiewicz, J., M. K. Gilson, I. H. Lee, and J. A. McCammon. 1995. Acetylcholinesterase: diffusional encounter rate constants for dumbbell models of ligand. *Biophys J.* 68:62–68.

Atkins, P. 1994. Physical Chemistry, 5th ed. W. H. Freeman & Co., New York.

Brenner, H. 1964a. The Stokes resistance of an arbitrary particle. II. An extension. *Chem. Eng. Sci.* 19:599–629.

Brenner, H. 1964b. The Stokes resistance of an arbitrary particle. III. Shear fields. *Chem. Eng. Sci.* 19:631–651.

Brune, D., and S. Kim. 1994. Hydrodynamic steering effects in protein association. *Proc. Natl. Acad. Sci. USA.* 91:2930–2934.

Davis, M. E., J. D. Madura, B. A. Luty, and J. A. McCammon. 1991. Electrostatics and diffusion of molecules in solution: simulations with the University of Houston Brownian Dynamics program. *Comput. Phys. Commun.* 62:187–197.

Deutch, J. M., and B. U. Felderhof. 1973. Hydrodynamic effect in diffusion-controlled reaction. *J Chem. Phys.* 59:1669–1671.

Ermak, D. M., and J. A. McCammon. 1978. Brownian dynamics with hydrodynamic interactions. *J. Chem. Phys.* 69:1352–1360.

Friedman, H. L. 1966. A hydrodynamic effect in the rates of diffusion-controlled reactions. *J. Phys. Chem.* 70:3931–3933.

Garcia de la Torre, J., and V. A. Bloomfield. 1977. Hydrodynamic properties of macromolecular complexes. I. Translation. *Biopolymers.* 16: 1765–1778.

Garcia de la Torre, J., and V. A. Bloomfield. 1981. Hydrodynamic properties of complex, rigid, biological macromolecules: theory and applications. *Q. Rev. Biophys.* 14:81–139.

Happel, J., and H. Brenner. 1973. Low Reynolds Number Hydrodynamics. Noordhoff International Publishing, Leyden.

Harvey, S. C., and J. Garcia de la Torre. 1980. Coordinate systems for modeling the hydrodynamic resistance and diffusion coefficients of irregularly shaped rigid macromolecules. *Macromolecules.* 13:960–964.

Head-Gordon, T., and C. L. Brooks III. 1987. The role of electrostatics in the binding of small ligands to enzymes. *J. Phys. Chem.* 91:3342–3349.

Luty, B. A., R. C. Wade, J. D. Madura, M. E. Davis, J. M. Briggs, and J. A. McCammon. 1993. Brownian dynamics simulations of diffusional encounters between triose phosphate isomerase and glyceraldehyde phosphate: electrostatic steering of glyceraldehyde phosphate. *J. Phys. Chem.* 97:233–237.

Madura, J. D., M. E. Davis, M. K. Gilson, R. C. Wade, B. L. Luty, and J. A. McCammon. 1994. Biological applications of electrostatic calculations and brownian dynamics simulations. *Rev. Comput. Chem.* 5:229–267.

McCammon, J. A., and S. C. Harvey. 1987. Dynamics of Proteins and Nucleic Acids. Cambridge University Press, Cambridge.

Northrup, S. H., S. A. Allison, and J. A. McCammon. 1984. Brownian dynamics simulation of diffusion-influence bimolecular reactions. *J. Chem. Phys.* 80:1517–1524.

Northrup, S. H., J. O. Boles, and J. C. L. Reynolds. 1987. Electrostatic effects in the Brownian dynamics of association and orientation of heme proteins. *J. Phys. Chem.* 91:5991–5998.

Oseen C. W. 1927. Neuere Methoden und Ergebnisse in der Hydrodynamik. Akademische Verlagsgesellschaft M. B. H., Leipzig, Germany.

Rotne, J., and S. Prager. 1969. Variational treatment of hydrodynamic interactions on polymers. *J. Chem. Phys.* 50:4831–4837.

Press, W. H., B. P. Flannery, S. A. Teukolsky, and W. T. Vetterling. 1986. Numerical Recipes. Cambridge University Press, Cambridge.

Teller, D. C., E. Swanson, and C. de Haën. 1979. The translational friction coefficient of proteins. *Methods Enzymol.* 61:103–124.

Wade, R. C., B. A. Luty, E. Demchuk, J. D. Madura, M. E. Davis, J. M. Briggs, J. A. McCammon. 1994. Simulation of enzyme-substrate encounter with gated active sites. *Nature Struct. Biol.* 1:65–69.

Wolynes, P. G., and J. M. Deutch. 1976. Slip boundary conditions and the hydrodynamic effect on diffusion controlled reactions. *J. Chem. Phys.* 65:450–454.

Yamakawa, H. 1970. Transport properties of polymer chains in dilute solutions: hydrodynamic interactions. *J. Chem. Phys.* 53:436–443.

Zwanzig, R. 1969. Langevin theory of polymer dynamics in dilute solution. *In* Stochastic Processes in Chemical Physics. K. E. Shuler, editor. Interscience Publishers, New York. 325–331.

Zwanzig, R., J. Kiefer, and G. H. Weiss. 1968. On the validity of the Kirkwood-Riseman theory. *Proc. Natl. Acad. Sci. USA.* 60:381–386.